Supporting Information

Tungsten Carbide Encapsulated in Grape-Like N-Doped Carbon Nanospheres: One-Step Facile Synthesis for Low-Cost and Highly Active Electrocatalysts in Proton Exchange Membrane Water Electrolyzers

Qi Feng [a, b, c], Yongyueheng Xiong [a], Linjing xie [a, c], Zhen Zhang [a, b], Xiner Lu [a], Yajun Wang [b, d], Xiao-Zi Yuan [e], Jiantao Fan [a, c], Hui Li [a, c *] and Haijiang Wang [c, d *]

a Department of Materials Science and Engineering, Shenzhen Key Laboratory of Hydrogen Energy, Southern University of Science and Technology, Shenzhen 518055, Guangdong, China

b School of Materials Science and Engineering, Harbin Institute of Technology, Harbin 150001, China

c Guangdong Provincial Key Laboratory of Energy Materials for Electric Power, Southern University of Science and Technology (SUSTech), Shenzhen 518055, China

d Department of Mechanical and Energy Engineering, Southern University of Science and Technology, Shenzhen, 518055, China

e Research Center of Energy, Mining and Environment, National Research Council Canada, 4250 Wesbrook Mall, V6T1W5, Canada

* Corresponding author: Department of Materials Science and Engineering, Southern University of Science and Technology, Shenzhen, 518055, China

E-mail address: hui.li@sustc.edu.cn, wanghj@sustc.edu.cn

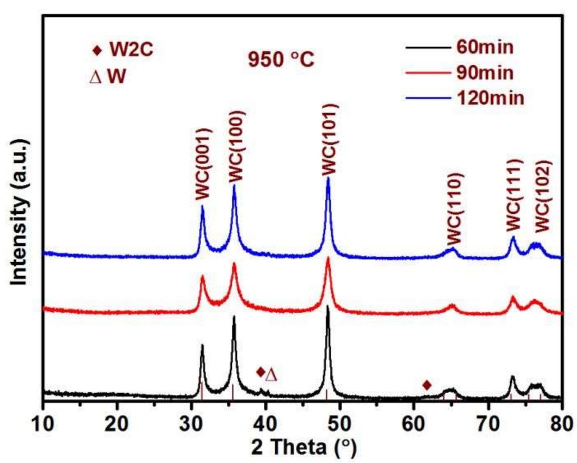

Figure S1. XRD patterns of as-synthesized WC@NC (4AMT) with different pyrolysis times at 950 °C.

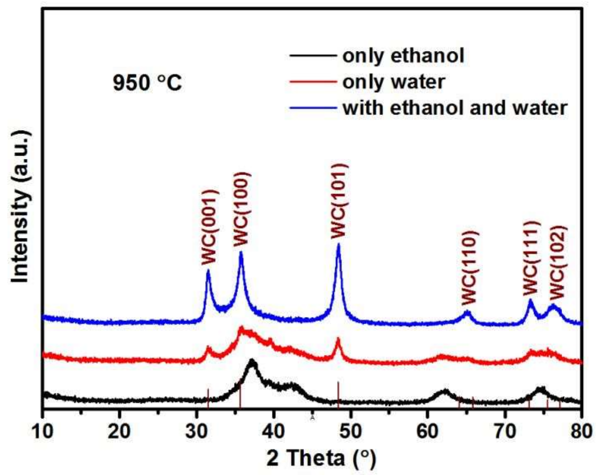

Figure S2. XRD patterns of as-synthesized WC@NC (4AMT) with different solvent ratios (water/ethanol) at 950 °C.

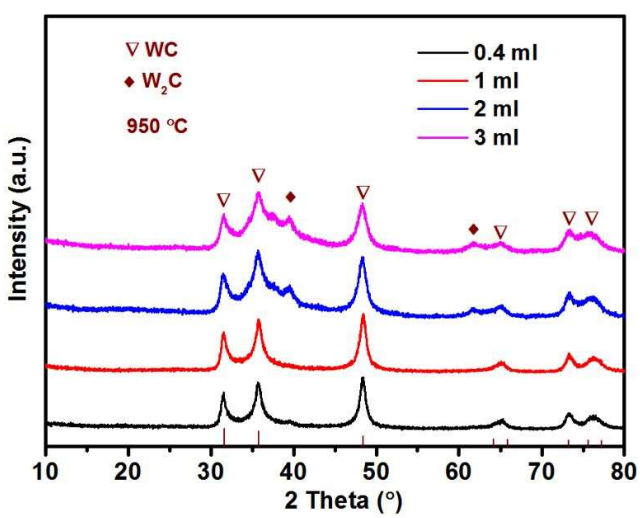

Figure S3. XRD patterns of as-synthesized WC@NC (4AMT) with different volumes (PH values) of $NH_3 \cdot H_2O$ at 950 °C.

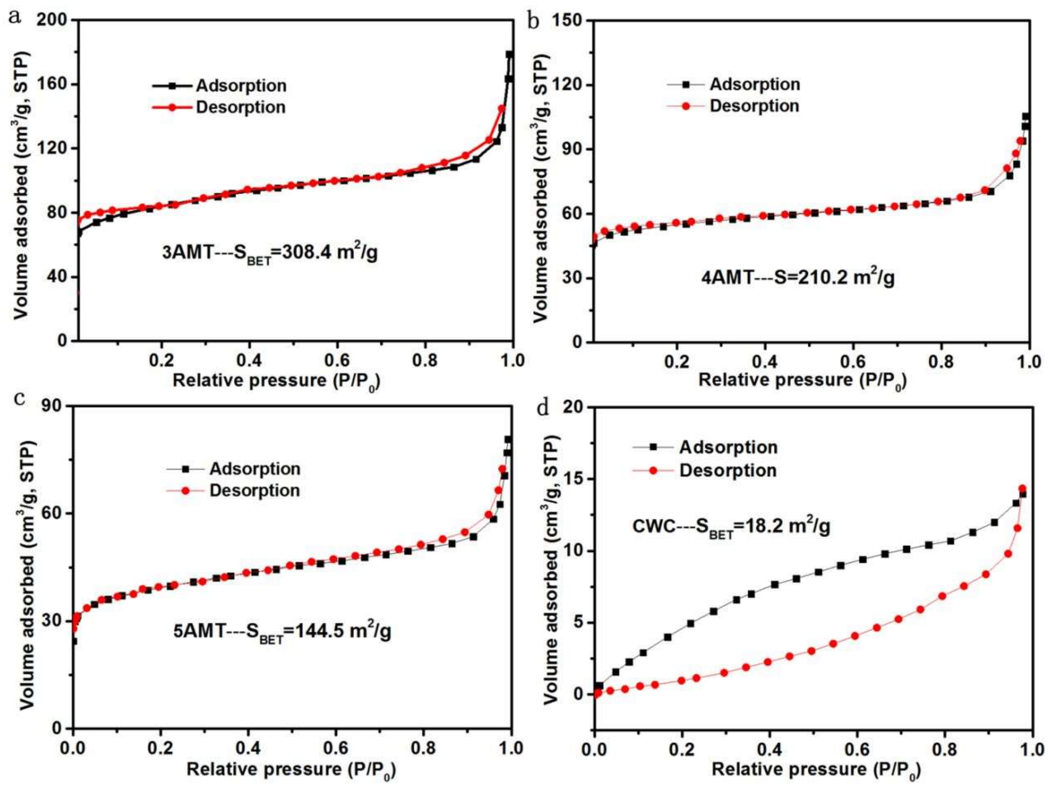

Figure S4. N_2 adsorption-desorption isotherm curves of (a) WC@NC (3AMT), (b) WC@NC (4AMT), (c) WC@NC (5AMT) and (d) commercial WC (CWC).

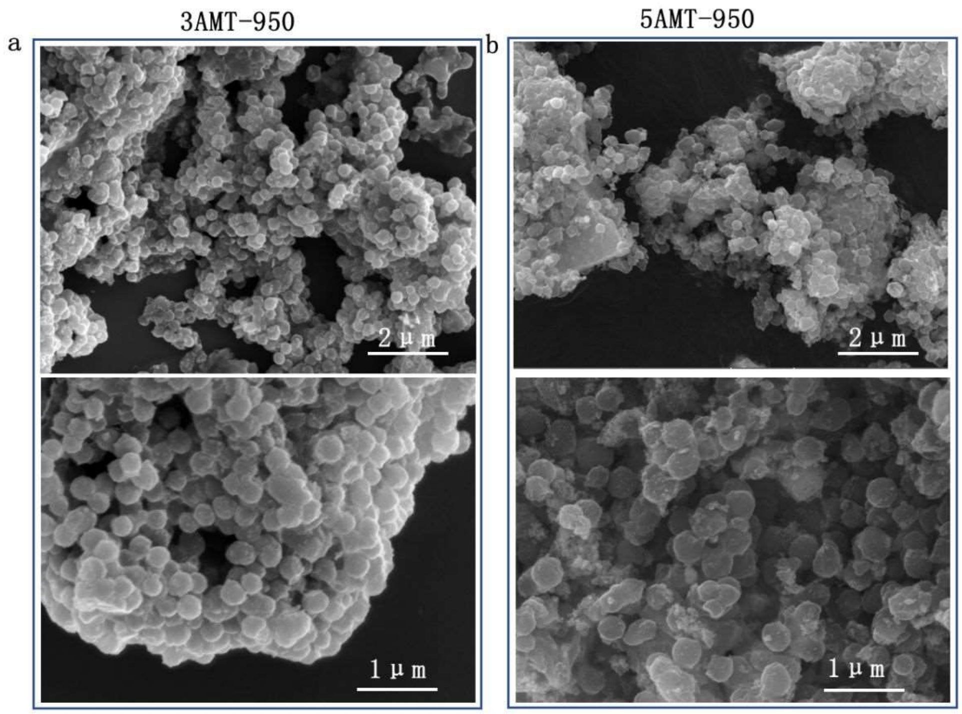

Figure S5. The influence of AMT/dopamine ratio: SEM images of (a) 3AMT and (b) 5AMT at 950 °C.

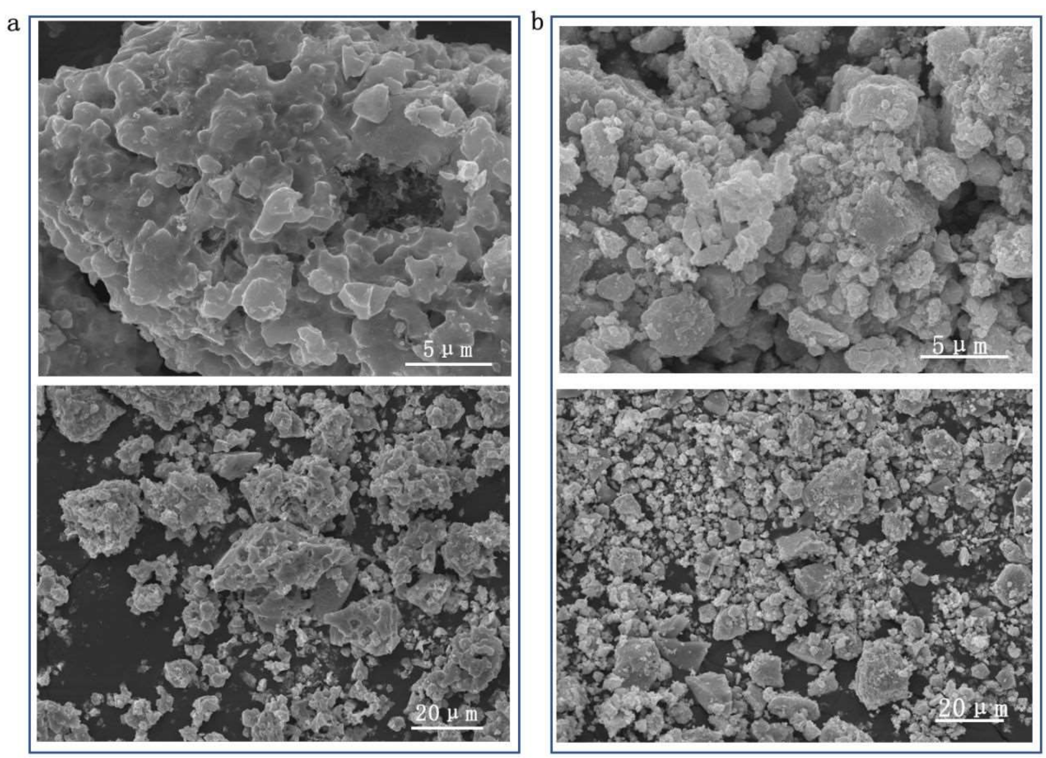
a
b
5 μm
20 μm
5 μm
20 μm

Figure S6. The influence of water/ethanol ratio: SEM images of 4AMT under the condition of (a) only ethanol with no water addition, (b) only water with no ethanol addition.

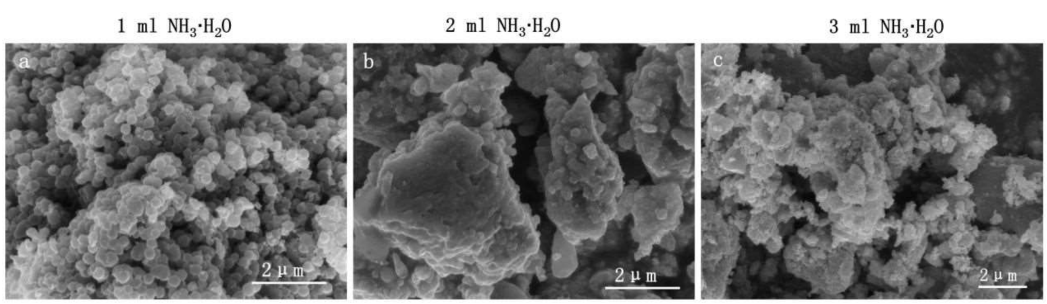

Figure S7. The influence of PH value: SEM images of 4AMT with (a) 1 mL

$NH_3 \cdot H_2O$, (b) 2 mL $NH_3 \cdot H_2O$, and (c) 3 mL $NH_3 \cdot H_2O$ at 950 °C.

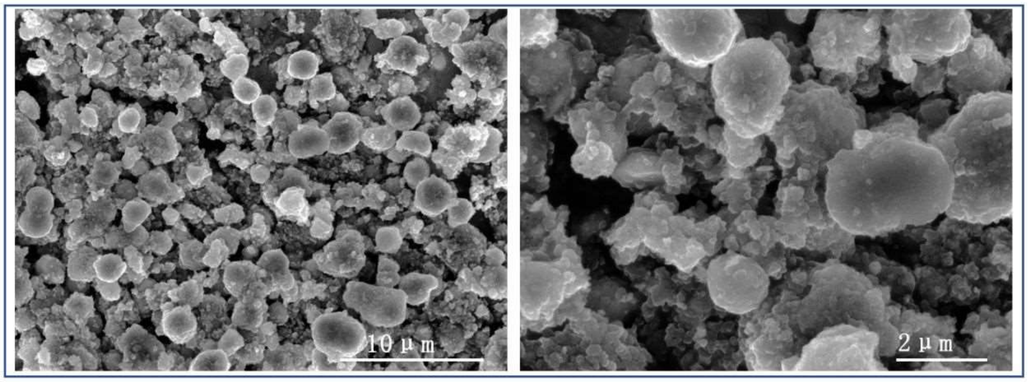

Figure S8. SEM images of 4AMT using Na_2WO_4 as tungsten source.

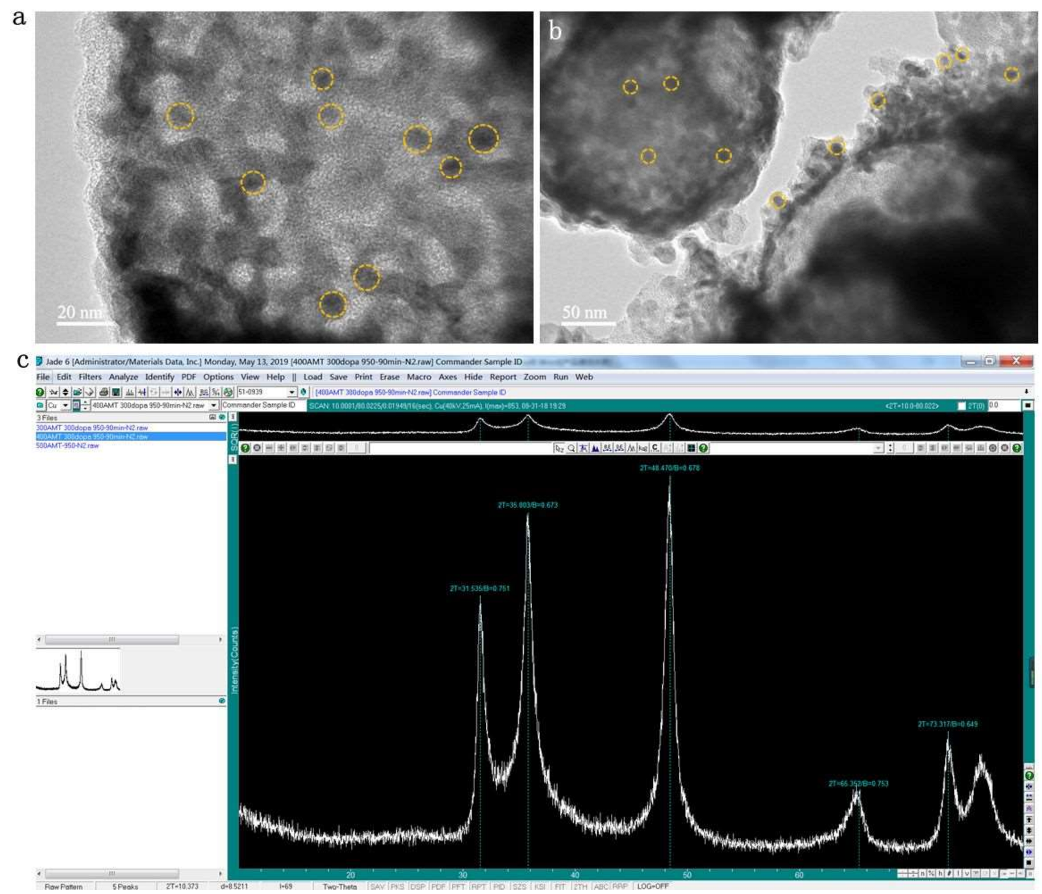

Figure S9. (a) low- and (b) high- magnified TEM images of 4AMT. (c) FWHM data and Bragg diffraction angle derived from the raw data in MDI Jade software.

Calculation of the WC grain size

A theoretical calculation results derived from the Scherrer Formula, which is well accordance with the WC grain size in TEM image. According to the Scherrer Formula, the grain size D can be calculated from the formula (S-1),

$$D = \frac{k\lambda}{B\cos\theta} \tag{S-1}$$

K=0.89, λ=0.154056 nm, B is the FWHM, and θ is the Bragg diffraction angle. The grain size was about 11.6 nm.

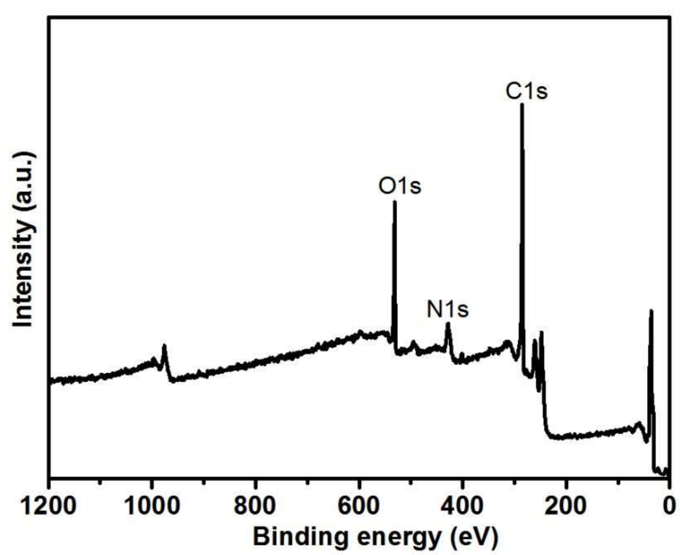

Figure S10. The full XPS spectra of WC@NC (4AMT).

Table S1. Comparison of HER activities for different electrocatalysts in 0.5 M H_2SO_4

Sample	η @ 10 mA cm^{-2} mV (vs. RHE)	Tafel slope (mV $decade^{-1}$)	ECSA (mF cm^{-2})
3AMT	165	76.7	13.1
4AMT	127	56.3	24.3
5AMT	152	68.4	20.6
CWC	243	103.4	7.2
Pt/C	27	31.3	-

Table S2. Comparison of HER activities for WC@NC with other tungsten carbides recently reported in 0.5 M H_2SO_4

Material	**electrolyte**	**Loading (mg cm^{-2})**	**η_{10} (mV)**	**Tafel slope (mV decade^{-1})**	**Reference**
WC@NC	0.5 M H_2SO_4	0.71	127	56.3	This work
WC_x/C	0.5 M H_2SO_4	0.45	154	65	Small Methods 2018, 2, 1700353
W_2C/CNT WC/CNT	0.5 M H_2SO_4	0.556	123 250	45 78	Nat. Commun., 2016, 7, 13216.
WC nanowalls	0.5 M H_2SO_4	-	160	67	Appl. Catal. B, 203 (2017) 684–691
W_2C/WC nanoparticles	0.5 M H_2SO_4	2.7	310	108	Appl. Catal. B, 236 (2018) 147–153
WC nanoarray	0.5 M H_2SO_4	16	89	75	Nat. Commun., 2018, 9, 924
Porous WC	0.5 M H_2SO_4	-	187.1	87.8	Nanoscale 2017, 9, 5413.

W_2C/graphic layer	0.5 M H_2SO_4	0.5	135	68	J. Mater. Chem. A 2016, 4, 8204
WC NPs	0.5 M H_2SO_4	1	125	84	ChemSusChem 2013, 6, 168
e-WCN	0.5 M H_2SO_4	0.4	220	47	Angew. Chem. Int. Ed., 2013, 52, 13638
porous WC film	0.5 M H_2SO_4	0.16	275	69	J. Mater. Chem. A, 2015, 3, 5798
WC-CNTs	0.5 M H_2SO_4	-	145	72	ACS Nano, 2015, 9, 5125
WCx/C	0.5 M H_2SO_4	1.05	264	85	ACS Appl. Mater. Interfaces 9 (2015) 20594–20602.
WC@NPC	0.5 M H_2SO_4	0.209	51	49	J. Am. Chem. Soc., 2017, 139 (15), pp 5285–5288
Mo_2C@NC	0.5 M H_2SO_4	0.5	180	51.3	Appl. Catal. B, 224 (2018) 533–540
Mo_2C-GNR	0.5 M H_2SO_4	0.2	152	65	ACS Nano, 2017, 11 (1), pp 384–394
N, P/Mo_2C@C	0.5 M H_2SO_4	0.9	141	56	ACS Nano 10 (2016) 8851–8860
Mo_2C nano-octahedra	0.5 M H_2SO_4	0.8	142	53	Nat. Commun. 6 (2015) 6512

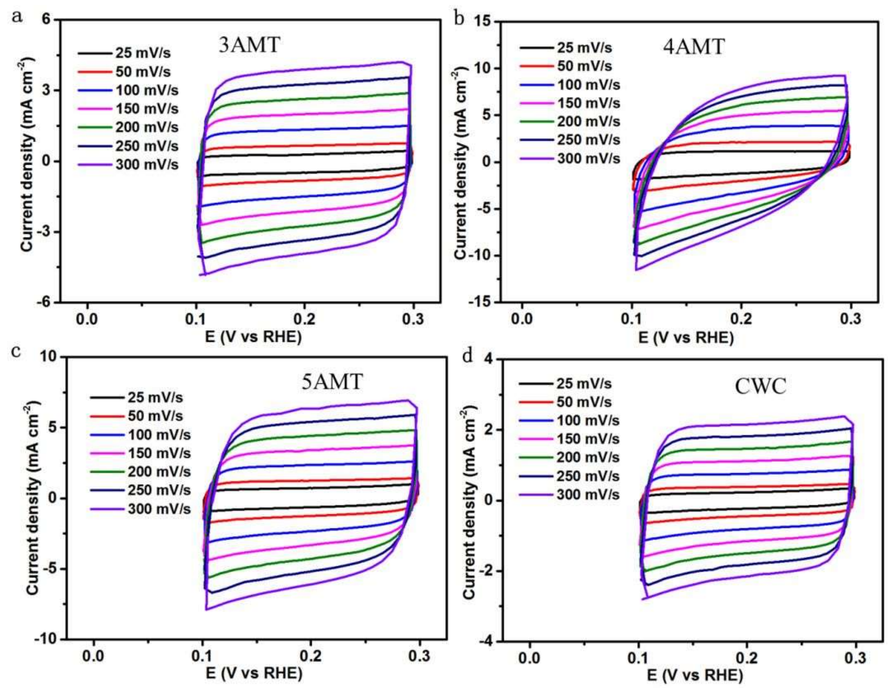

Figure S11. Cyclic voltammogram curves of (a) WC@NC (3AMT), (b) WC@NC (4AMT), (c) WC@NC (5AMT), and (d) CWC with different scanning rates from 25 to 300 mV s^{-1} over a potential range of 0.1-0.3 V vs. RHE in 0.5 M H_2SO_4.

Table S3 EIS analysis at -0.25 V for 3AMT, 4AMT, 5AMT and CWC catalysts

Catalysts	Rs	Rp	CPE1-T	CPE1-P	Rct	CPE2-T	CPE2-P
3AMT	5.02	1.5	0.017	0.45	8.1	0.004	0.85
4AMT	5.07	1.3	0.012	0.61	5.1	0.006	0.80
5AMT	5.13	1.3	0.009	0.53	7.4	0.005	0.78
CWC	5.04	5.0	0.008	0.53	13.0	0.001	0.84

*: CPE-P is the Constant Phase Element-P, which is related to the semicircle in the Nyquist plot, and CPE-T is the Constant Phase Element-T, which is the pseudo capacitance.

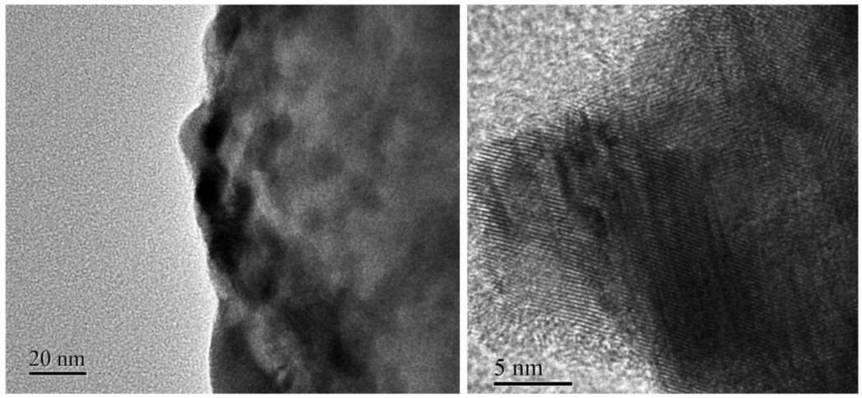

Figure S12. TEM images after 9 h chronoamperometry stability test for sample 4AMT

Table S4. Comparison of the PEMWE operation in this work with results from previous reports

Reference	Cathode	Anode	Cell temperature (°C)	Current density at 2 V (A/cm^2)
This work	WC/C	IrO_2	80	0.78
Int J Hydrogen Energy 2014, 39 (35), 20837-20843	MoS_2/RGO	IrO_2	80	0.35
ACS Catalysis 2016, 6 (4), 2626-2631.	FeS_2/C	IrO_2	90	0.61
Appl Catal B-Environ 2018, 232, 93-100.	$Ni_{0.64}Co_{0.36}O_xS_{0.14}$/CP	IrO_2/CP	90	0.72
Appl Catal B-Environ 2017, 206, 608-616	$Cu_{93.7}Mo_{0.63}$/CP	IrO_2/CP	90	0.73
J. Power Sources 2018, 392, 69-78.	MoS_x/CP	IrO_2/CP	90	0.54
Small 2016, 12 (40), 5530-5537	$MoS_{1.7}$/CC	RuO_2/CP	45	0.30

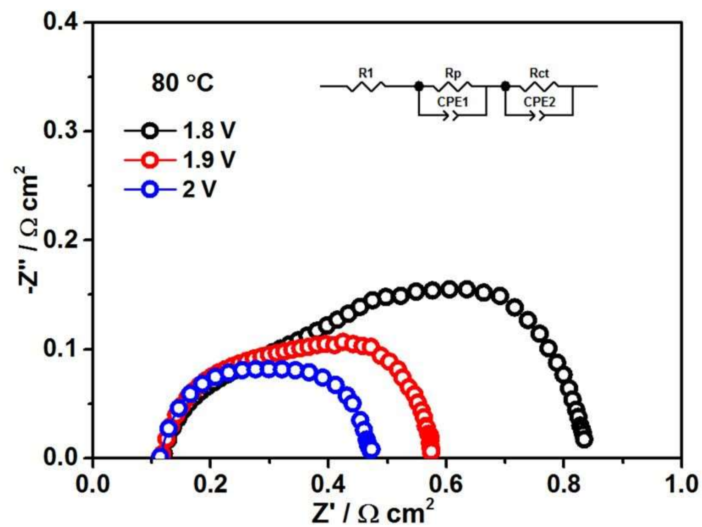

Figure S13. EIS curves of the PEM electrolyzer using WC@NC (4AMT) as cathode at applied cell voltages of 1.8, 1.9 and 2.0 V at 80°C. The fitting results have been listed in table S3. R_1 is the ohmic resistance, CPE represents the constant phase elements, the resistance related to the catalyst layer is depicted with Rp, and the polarization resistance is Rct.

Table S5 EIS analysis for the PEM electrolyzer derived from Figure S13

Applied votage (V)	R_1 (Ω cm^2)	Rp (Ω cm^2)	CPE1-T	CPE1-P	Rct (Ω cm^2)	CPE2-T	CPE2-P
1.8	0.12	0.18	0.08	0.25	0.49	0.277	0.663
1.9	0.13	0.15	0.053	0.634	0.31	0.207	0.654
2	0.13	0.12	0.052	0.634	0.24	0.215	0.649

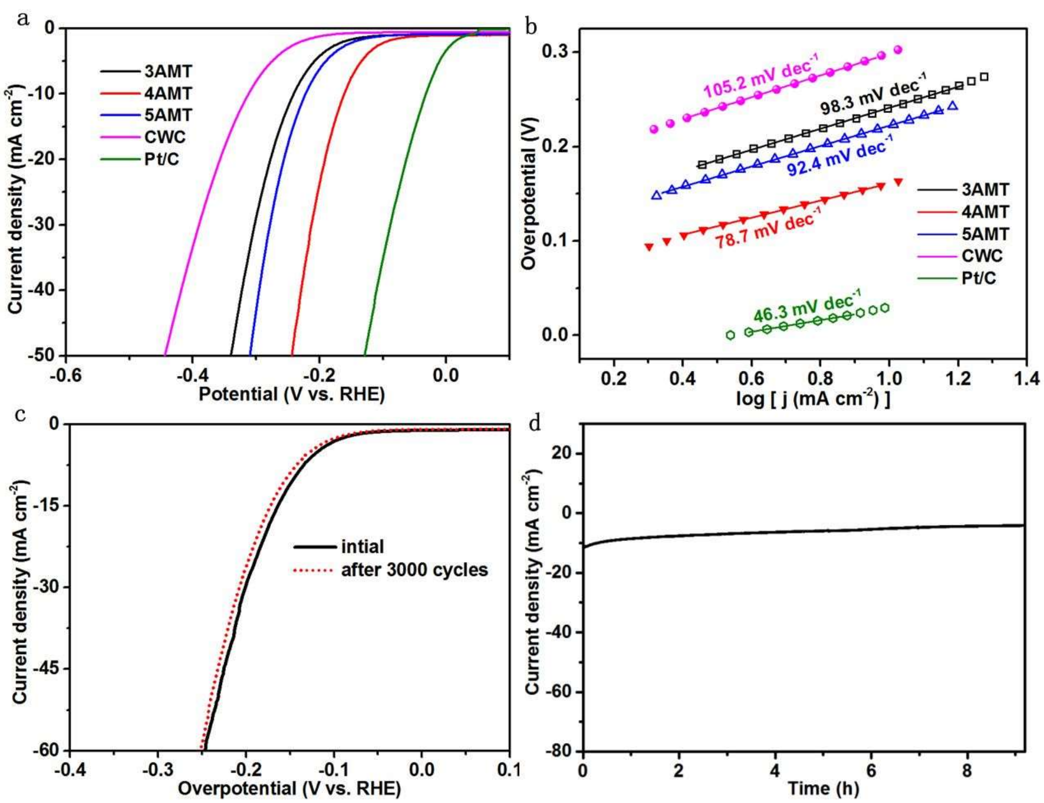

Figure S14. (a) Polarization curves of 3AMT, 4AMT, 5AMT, Pt/C and CWC in 1 M KOH at 5 mV s^{-1}. (b) Tafel plots calculated from (a). (c) Polarization curves of 4AMT before and after 3000 CV cycles in 1 M KOH at 5 mV s^{-1}. (d) Time-dependent current density curve at −0.147 V (vs. RHE) of 4AMT in 1 M KOH.

Table S6. HER activities of different electrocatalysts in 1 M KOH

Sample	η @ 10 mA cm^{-2} mV (vs. RHE)	Tafel slope (mV $decade^{-1}$)
3AMT	239	98.3
4AMT	141	78.7
5AMT	217	92.4
CWC	312	105.4
Pt/C	32	46.3

Table S7. Comparison of HER activities for WC@NC with literature recently reported in alkaline media

Material	electrolyte	Loading (mg cm^{-2})	η_{10} (mV)	Tafel slope (mV dec^{-1})	Reference
WC@NC	1 M KOH	0.71	141	78.7	This work
Mo_2C nano-octahedra	1 M KOH	0.8	151	59	Nat. Commun. 6 (2015) 6512
WC_x/C	1 M KOH	0.45	262	115	Small Methods 2018, 2, 1700353
Porous WCx nanowires	1 M KOH	1.08	122	56	J. Mater. Chem. A, 2017, 5, 13196
TCNC (WC)	1 M KOH	-	300	133	ChemSusChem 2016, 9, 2784.
WC-CNTs	0.1 M KOH	-	137	106	ACS Nano, 2015, 9, 5125
Co_2P/WC@NC	1 M KOH	1.06	180	91	ChemSusChem, 2018, 11, 1082.

Mo_2C/NC	1 M KOH	0.5	110	49.7	Appl. Catal. B, 224 (2018) 533–540

DFT Calculations for HER

We calculated the theoretical models for graphene, N-graphene, WC, WC@graphene, and WC@N-graphene, as shown in Figure S15. For the adsorption sites of H*, we obtained the most stable configurations after efforts with different adsorption sites, including the hollow sites, bridge sites and top sites, also shown in Figure S15.

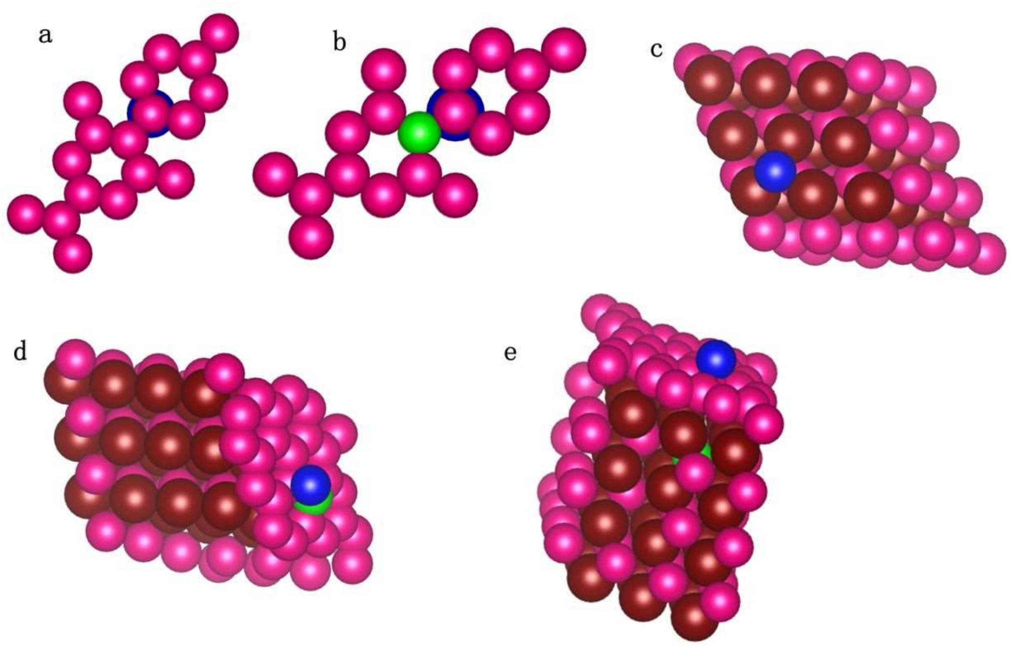

Figure S15. The theoretical models used in DFT calculations and the adopted adsorption sites of H* on the surface of these models: (a) C, (b) NC, (c) WC, (d) WC@CN and (e) WCN@C, where the pink spheres represent carbon atoms; the brown spheres imitate tungsten atoms;the green spheres stand for nitrogen atoms; and the blue spheres correspond to hydrogen atoms.

Note that our calculations followed the proposed method by Norskov et al. (J.

Am. Chem. Soc. 127 (2005) 5308-5309). Spontaneously, the adsorption free energy of H* is derived from the following equation (S-2):

$$\Delta G_{H^*} = \Delta E_{H^*} + \Delta E_{ZPE} - T\Delta S \tag{S-2}$$

where ΔE_{H^*}, ΔE_{ZPE}, and ΔS denote the adsorption energy, the change of the zero-point energy, and entropy change of the adsorbed hydrogen on the surface, respectively.

Firstly, the adsorption energy (ΔE_H) for hydorgen on surface can be defined by (S-3)

$$\Delta E_H = 1/n[E(slab + nH) - E(slab) + n/2E(H_2)] \tag{S-3}$$

where E(slab+nH), E(slab), and E(H_2) are the energies of the slab model with n hydrogen adsorbed on, the perfect slab model, and the H_2, respectively. Secondly, the change of the zero-point energy (ΔE_{ZPE}) can be derived from the phonon vibration. Finally, the change of the entropy (ΔS_{H2}) of the adsorbed hydrogen on surface can be expressed as follows (S-4):

$$\Delta S_{H2} \approx -1/2S^0_{H_2} \tag{S-4}$$

where S^0_{H2} is the entropy of the hydrogen adsorption under the standard condition, which is about 130.694 J (K mol)$^{-1}$. At a system temperature of 300 K, the value of TΔS is calculated to be −0.2 eV, which is in agreement with the previous report (Angew. Chem., Int. Ed. 2015, 54, 10752−10757). Therefore, the free energy of the adsorbed state of hydrogen on the surface can be calculated as follows (S-5),

$$\Delta G^*_H = \Delta E_H + \Delta E_{ZPE} + 0.2eV \tag{S-5}$$

The free energies of the adsorbed states are listed in Table S7.

Table S8. The adsorption energy of H species (ΔE_{H*}), the relevant contributions to the free energy (ΔZPE and $T\Delta S$), and the free energy of adsorbed H* ($\Delta GH*$) on different surfaces.

Models	ΔE_{H*} (eV)	ZPE_{H*} (eV)	ΔZPE (eV)	ΔG_{H*} (eV)
C	1.473	0.285	0.148	1.82
NC	0.34	0.314	0.176	0.72
WC	-0.654	0.167	0.028	-0.56
WC@NC	-0.515	0.312	0.175	-0.14
WCN@C	-0.543	0.313	0.174	-0.17